PHYSICAL REVIEW B, VOLUME 63, 121302(R)

Raman scattering in strongly coupled organic semiconductor microcavities

A. I. Tartakovskii,[1,2] M. Emam-Ismail,[2] D. G. Lidzey,[2] M. S. Skolnick,[2] D. D. C. Bradley,[2]
S. Walker,[3] and V. M. Agranovich[4]
[1]*Institute of Solid State Physics, Russian Academy of Sciences, 142432 Chernogolovka, Russia*
[2]*Department of Physics and Astronomy, University of Sheffield, Sheffield S3 7RH, United Kingdom*
[3]*Department of Electronic and Electrical Engineering, University of Sheffield, Sheffield S1 3JD, United Kingdom*
[4]*Institute of Spectroscopy, RAS, 142190 Troitsk, Russia*
(Received 2 November 2000; published 5 March 2001)

We report the observation of resonant Raman scattering in the strong coupling regime for a planar microcavity containing cyanine dye *J* aggregates. The giant Rabi splitting between the polariton branches, resulting from the very large exciton oscillator strengths, allows the observation of doubly resonant Raman scattering where both incident and scattered photons are in resonance with the mixed exciton-cavity-mode states. Under double resonance conditions the Raman signals are found to be very significantly enhanced, by factors up to 300, relative to noncavity organic films.

DOI: 10.1103/PhysRevB.63.121302 PACS number(s): 78.30.Jw, 78.55.Kz, 71.36.+c

Microcavities (MC's) strongly modify the spectral and spatial distribution of photon fields in solid state systems and as a result lead to major changes in the nature and efficiency of light-matter interaction processes. One of the manifestations of such modifications is the occurrence of the strongly coupled exciton-photon modes termed cavity polaritons.[1] The strong coupling regime has been achieved and studied in detail for inorganic semiconductor microcavities at low temperatures where the damping of excitons is smaller than the characteristic (Rabi) splitting of polariton modes (usually <10 meV).[1] Very recently strong coupling has been demonstrated for organic microcavities containing porphyrin[2] and cyanine dyes.[3,4] Giant Rabi splittings up to 160 meV, resulting from the very large oscillator strengths of the Frenkel excitons in the organic materials, have been reported from room temperature reflectivity and photoluminescence (PL) measurements. The very strong exciton-photon coupling, and hence high polariton stability, in combination with the small polariton density of states[6] and high phonon scattering rates relative to inorganics[2,5] are likely to favor the observation of bosonic nonlinear effects, currently of very high topicality for inorganic structures.[7]

Another class of effects arising due to the novel aspects of the light-matter interaction in microcavities is the modification of the efficiency of Raman processes. Strong enhancements of Raman scattering efficiency due to photon field confinement have been reported for various kinds of cavity geometries and materials—for example, for CCl_4 micron-size droplets,[8] for liquid benzene in piezoelectrically controlled Fabry-Perot cavities,[9] and for high-finesse Fabry-Perot semiconductor microcavities with embedded quantum wells in both III-V (Refs. 10–12), and II-VI (Ref. 13) material systems. In Ref. 10, purely optical enhancement of LO-phonon Raman scattering efficiency was reported, whereas in Refs. 11–13 polariton-mediated resonant Raman scattering was discussed in detail. The authors concentrated mostly on single-resonance experiments[12,13] in which evidence for the role of polaritons as intermediate states in the scattering process was presented. By contrast, the conditions for doubly resonant Raman scattering (i.e., when both incident and scattered photons are in resonance with polariton states) are not easily achievable for inorganic microcavities since the energy of optical phonons is much larger than achievable magnitudes of Rabi splittings.[14] As a result the doubly resonant Raman experiments which have been reported were performed for conditions where either ingoing or outgoing channels were of pure photon character.[11]

In the present Rapid Communication, we report the observation of resonant Raman scattering in the strong coupling regime in microcavities containing cyanine dye *J* aggregates. The giant Rabi splitting allows doubly resonant Raman scattering experiments to be performed where the energies of both incident and scattered photons coincide with those of strongly mixed exciton-photon states. The double-resonance conditions are probed by tuning of both the angle of detection and the energy of the exciting laser. The difference observed in the width of the Raman profiles in the two cases is explained in terms of the respective variations of the ingoing and outgoing transmission functions for the two types of experiment. A strong enhancement of the Raman signal is found by comparison with that observed from the same films but outside a microcavity.

The microcavity samples used in our investigations were fabricated on a high-reflectivity dielectric Bragg mirror consisting of nine alternating $\lambda/4$ pairs of Si_xN_y and SiO_2 (peak reflectivity of 98% at 690 nm) deposited on a quartz substrate. A 180-nm-thick layer of the cyanine dye dispersed in a polyvinyl alcohol (PVA) matrix was deposited by spin coating on the dielectric mirror and a silver mirror was then evaporated on the organic film to complete the microcavity. We also studied noncavity PVA matrix films containing cyanine dyes (of the same thickness, 180 nm, as those in microcavities) spin-coated onto a quartz substrate. The *J* aggregates used in our work have a peak absorption at 1.85 eV with linewidth ≈ 50 meV.[15] The angle-resolved PL and Raman scattering experiments were performed using HeNe and tunable cw Ti-sapphire lasers. A projector lamp was employed for reflectivity characterization. The samples were placed in the vacuum space of a cryostat with wide angular access. Experiments were carried out over the temperature range 60–300 K. The reflectivity, PL, and Raman signals were detected using a charge-coupled device (CCD) detector coupled with a 50-cm single spectrometer.

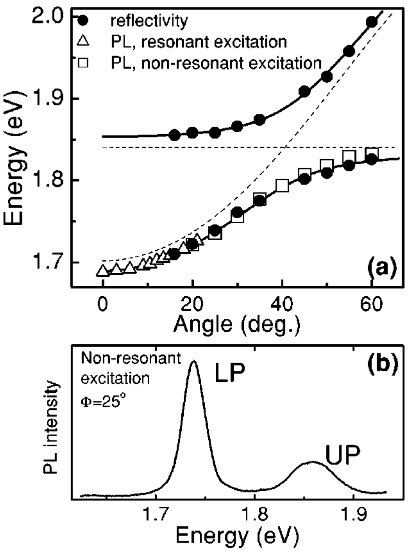

FIG. 1. (a) Polariton mode dispersion measured from reflectivity (circles) and PL (squares and triangles for nonresonant and resonant excitation into the LP branch, respectively). The calculated polariton (uncoupled photon and exciton) dispersion is shown by the solid (dashed) lines. (b) PL spectrum recorded at $\Phi = 25°$ for nonresonant excitation. Lower and upper polariton peaks are denoted as LP and UP, respectively.

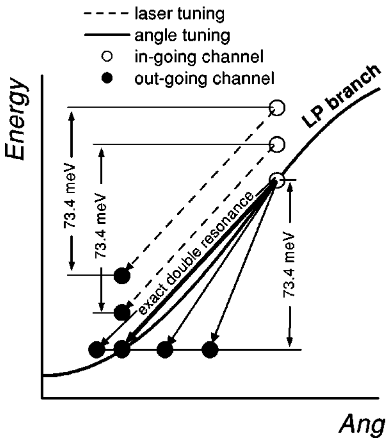

FIG. 3. Schematic diagram of the resonant Raman scattering experiments.

Solid symbols in Fig. 1(a) show the polariton dispersion obtained from the angle-resolved reflectivity measurements at 300 K (the angle of detection, Φ, is measured from the normal to the sample surface). A large Rabi splitting $\Omega = 88$ meV is deduced from fitting of the dispersion curve (solid lines) to a simple two-level exciton-cavity model. From the fitting it is deduced that this particular sample has a small negative detuning $\Delta = E_C(\Phi = 0) - E_X(\Phi = 0)$ of uncoupled cavity (C) and exciton (X) modes of order 1.6Ω. The same dispersion is also deduced from the PL studies [open symbols in Fig. 1(a)]. When using nonresonant high-energy excitation (with a HeNe laser at $E_{HeNe} \approx 1.95$ eV), the PL at room temperature close to $\Phi \approx \Phi_{res}$ [Φ_{res} is determined by $E_C(\Phi_{res}) - E_X(\Phi_{res}) \approx 0$] is observed only from the lower polariton branch since emission from the upper branch is suppressed due to rapid relaxation of the polaritons to lower-energy states.[3] However, for negative detuning for $\Phi < \Phi_{res}$, as the exciton fraction of the lower branch decreases, relaxation into the lower branch states becomes less probable,[16] with the result that the two-peaked spectrum is seen. This is shown in Fig. 1(b) where a nonresonantly excited PL spectrum at 300 K and $\Phi = 25°$ for the same negative detuning as Fig. 1(a), is presented. Two peaks with linewidths of about 25 (LP) and 50 (UP) meV are observed.

Additional features appear in the spectrum when resonant excitation into the lower polariton branch is employed using a tunable Ti-sapphire laser.[17] In these measurements the laser beam is incident on the sample surface at a particular angle $\Theta = 34°$ [see the Fig. 2(a) inset], and the energy of the incident photons is fixed to the energy of the polariton state at that angle (with $k = \omega/c \sin\Theta$, where ω is the photon frequency). Figure 2(a) shows a series of spectra recorded at $T = 120$ K at various angles of detection, Φ, under these conditions of resonant excitation [the energies of the PL maxima are plotted as the open triangles in Fig. 1(a) (Ref. 18)]. In contrast to the case of nonresonant excitation additional very sharp features are observed in the spectra at 1.698 and 1.699 eV. Most importantly their energies are independent of the collection angle, with the strongest sharp line occurring at an energy of 73.4 meV below the laser line. The conditions realized in this experiment are shown schematically in the diagram of Fig. 3 by solid arrows.

To determine the origin of the sharp peaks, spectra were then recorded for fixed angles of excitation and detection, but varying the energy of the laser, thus tuning it through

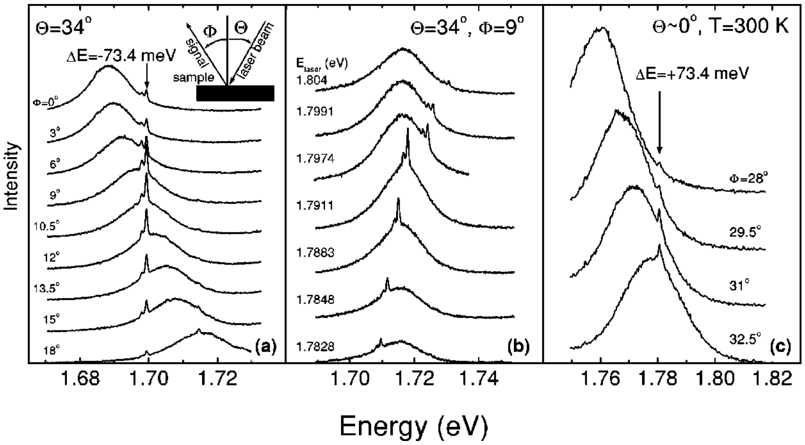

FIG. 2. (a) and (b) LP emission spectra recorded at 120 K for resonant excitation into the LP branch at $\Theta = 34°$. (a) Detection at $0 \leqslant \Phi \leqslant 18°$; E_{laser} is constant. (b) Detection at $\Phi = 9°$; E_{laser} is varied. (c) Excitation at $\Theta \approx 0°$ detection at $28° \leqslant \Phi \leqslant 32.5°$ at 300 K; E_{laser} is constant.

resonance with the LP branch. Such spectra recorded at $T = 120$ K are presented in Fig. 2(b). In this experiment the LP PL peak energy is constant, since the angle of detection is fixed. By contrast, the energies of the sharp lines superimposed on the much broader PL peak depend strongly on the laser energy. The energy separation between these peaks and the laser is constant with a separation below the laser line of $(-)73.4$ meV being found for the strongest line. The laser tuning experiment is represented in the diagram of Fig. 3 by the dashed arrows.

The constant energy separation from the laser energy, independent of laser energy and angle of detection, provides strong evidence that the sharp features arise from an inelastic scattering process—namely, Raman scattering. Further evidence to support this conclusion is presented in Fig. 2(c). The figure shows polariton emission spectra recorded at high temperature 300 K under conditions of resonant excitation into the LP branch at $\Theta \approx 0°$ at an energy of 1.707 eV. Here PL emission is now observed at energies up to nearly 80 meV above the excitation energy, due to the large thermal energy of equilibrium polaritons at 300 K. Surprisingly, a relatively weak sharp feature is observed at 1.781 eV—i.e., at an energy $+73.4$ meV above the laser energy. This sharp feature arises from anti-Stokes Raman scattering, the phonon population being sufficient at 300 K to allow the anti-Stokes companion of the Stokes features observed at lower temperature in Figs. 2(a) and 2(b) to be detected. The combination of the results in Figs. 2(a), 2(b), and 2(c) thus provides firm evidence for the attribution of the sharp features observed to Raman scattering processes.

It is important to note that in contrast to inorganic microcavities where strong coupling effects are only easily observed at $T < 100$ K due to the small exciton binding energies and Rabi splittings, the polaritons in organic structures are stable at room temperature and above. This high-temperature stability permits the observation of the anti-Stokes resonant Raman process in a strongly coupled microcavity.

Comparison of the above results with Raman spectra measured from a noncavity sample (PVA film containing cyanine dye) shows very close agreement between the energies measured in the two cases. The two peaks discussed above and many other Raman features (energies in the range from tens to hundreds of meV) from the monomer vibrational modes of cyanine dyes are discussed elsewhere in the literature.[19] Here we only present detailed results for the strongest Raman features.

As clearly seen in Figs. 2(a) and 2(b) the intensities of the Raman signals depend strongly on the relative energies of the polariton PL features and the Raman lines. In both Figs. 2(a) and 2(b), the Raman intensities are maximum when the lines are in resonance with the polariton emission peaks. In Fig. 2(a), the excitation is in resonance with the polariton branch at 34°. Thus for detection at 10.5° where the Raman intensity is maximum, both incident and scattered photon energies coincide with specific lower polariton branch states, and thus the double-resonance condition is achieved (the thick arrow in the diagram of Fig. 3). Similarly for Fig. 2(b), where the laser energy is tuned, the maximum in Raman intensity is found when both the laser and scattered photons are resonant with the polariton dispersion curves. Based on these results, we now plot the resonant Raman profiles shown in Fig. 4, where the intensity of the Raman features is plotted as a function of the energy difference (ΔE_{DR}) between the observed Raman signal and the energy for which exact double resonance is obtained. The circles represent the results of Fig. 2(a) when the ingoing channel is held constant and the outgoing channel is probed by tuning the detection angle. In contrast, for Fig. 2(b), where the laser energy is tuned (triangles in Fig. 4) both ingoing and outgoing resonance conditions are changed. It is notable in Fig. 4 that the Raman profile for the case of angle tuning is broader than that where the laser energy is varied. The observed difference can be easily understood on the basis of a simplified analysis using the expression for the cross section of polariton-mediated Raman scattering:[11–13,20] $\sigma_{pol} \propto T_i P_{phonon} T_s$. Here T_i and T_s are transmission functions for the incident and scattered photons, respectively. P_{phonon} is the probability of phonon-mediated scattering between initial and final polariton states, proportional to their exciton fractions. Here the scattering process is treated as the result of three successive steps: (i) transmission of a photon into the sample and conversion to a polariton, (ii) phonon-mediated scattering from one polariton state to another, and (iii) subsequent propagation and transmission of the scattered polariton and conversion to an external photon.

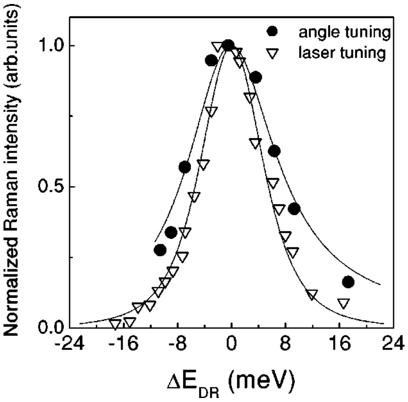

FIG. 4. Resonant Raman profiles relative to the double-resonance condition obtained using angle (circles) and laser (triangles) tuning. The lines show the curves calculated using equation for Raman efficiency presented in text.

In the case of angle tuning [Fig. 2(a)], T_i is held constant while T_s and P_{phonon} are varied. Over the range of angles studied, the change in σ_{pol} due to the change in P_{phonon} is relatively small $[P_{phonon}(\Phi = 21°) \approx 1.4 P_{phonon}(\Phi = 0°)]$, and thus the angle tuning can be considered effectively as a filter function (corresponding to the polariton transmission function) being scanned in energy, leading to a variation in the conversion efficiency of the scattered polariton into an external photon. The Raman profile in this case is thus determined mainly by the variation of $T_s(\Delta E_{DR})$. In the case of laser tuning P_{phonon} is constant since the same two polariton states are always probed. However, both T_i and T_s are varied. In this case, both incident and scattered photons are filtered by the polariton transmission functions. The profile obtained from the laser tuning experiment is thus proportional to $T_s(\Delta E_{DR})\times T_i(\Delta E_{DR})$. To describe $T(\Delta E_{DR})$ we have used Lorenzian functions. In order to fit the experimental results, Lorenzians with full widths at half maximum (FWHM) of 16 and 18 meV were employed for T_s and T_i, respectively. The results of the fitting are shown by the lines in Fig. 4. The magnitude of the fitting parameter for T_s is in good agreement with the width of the PL detected at small Φ ($\approx$15 meV), providing confidence in the procedure.[21] It is also notable that to obtain a good fit to the Raman profile in the case of the laser tuning a larger linewidth for T_i of 18 meV had to be used. This is consistent with the increase of the PL linewidth with Φ observed due to the stronger mixing of the cavity mode with the broader exciton mode at higher angle.[3]

As discussed above, the modification of light-matter interactions achieved in microcavities is expected to lead to significant enhancement of Raman efficiencies compared to the same films outside a microcavity. To investigate this we recorded Raman spectra from noncavity PVA films containing cyanine dye *J* aggregates using Ti-sapphire laser excitation tuned to an energy close to that used in the experiments above. The Raman scattering efficiency in the microcavities (characterized by a finesse $Q\approx 50$) under double-resonance conditions was found to be about 300 times larger than that for the noncavity sample. The enhancement of the Raman efficiency depends on the relative location and spatial extent of the active media and the maximum of the photonic field in the structure. Enhancements up to 10^4 were reported for high-finesse inorganic samples ($Q\approx 300$ and 2000),[10,22] 10^3 enhancement was reported for a $Q\approx 250$ cavity containing liquid benzene,[9] and 80 was found for an inorganic half cavity ($Q\approx 45$).[22] We thus conclude that the enhancement factor obtained from our experiments is in reasonable agreement with those reported previously.

The cavity-induced enhancement of the efficiency of the Raman scattering observed in our experiments is particularly interesting for investigations of nonlinear Raman processes. Recent studies of resonant Raman scattering in conjugated polymer thin films have exhibited nonlinear character under high-power pulsed laser excitation.[23] Although the threshold for nonlinear Raman gain was about one order of magnitude larger than that for spectrally narrowed emission, the slope of the Raman amplification was significantly steeper. The strong enhancements of Raman efficiencies found in the present work suggest very interesting possibilities for investigations of organic microcavities under resonant pulsed excitation. The high potential of such experiments is further supported by the fact that emission from *J* aggregates can show superradiance.[24]

In conclusion, doubly resonant Raman scattering mediated by polariton states has been observed in organic semiconductor microcavities with active regions formed from *J*-aggregated cyanine dye molecules. The Raman process is identified as arising from inelastic light scattering involving vibrational modes of the *J* aggregates. The Raman signals from the microcavities have been found to be up to 300 times stronger than for the same organic layers outside a cavity. The present results point the way to possibilities for the investigation of nonlinear Raman processes in strongly coupled microcavities using high levels of resonant pulsed laser excitation.

Financial support from EPSRC, EOARD, EC RTN Clermont HPRN-CT-1999-00132, and the Royal Society is gratefully acknowledged. A.I.T. is also grateful to the Russian Foundation for Basic Research and program ‘‘Fundamental spectroscopy’’ of the Russian Ministry of Science and Technology. D.G.L. thanks the UK EPSRC for support.

---

[1] M. S. Skolnick *et al.*, Semicond. Sci. Technol. **13**, 645 (1998).

[2] D. G. Lidzey *et al.*, Nature (London) **395**, 53 (1998).

[3] D. G. Lidzey *et al.*, Phys. Rev. Lett. **82**, 3316 (1999).

[4] D. G. Lidzey *et al.*, Science **288**, 1620 (2000).

[5] V. Agranovich, H. Benisty, and C. Weisbuch, Solid State Commun. **102**, 631 (1997).

[6] The refractive index of the organic film determining the E-k photon-mode dispersion is $\approx$1.6–1.7, thus leading to a polariton density of states about 3 times smaller than in inorganic microcavities.

[7] A. I. Tartakovskii *et al.*, Phys. Rev. B **60**, R11 293 (1999); P. G. Savvidis *et al.*, Phys. Rev. Lett. **84**, 1547 (2000); R. M. Stevenson *et al.*, *ibid.* **85**, 3680 (2000); A. I. Tartakovskii, D. N. Krizhanovskii, and V. D. Kulakovskii, Phys. Rev. B **62**, R13 298 (2000).

[8] Shi-Xiong Qian and Richard K. Chang, Phys. Rev. Lett. **56**, 926 (1986).

[9] F. Cairo *et al.*, Phys. Rev. Lett. **70**, 1413 (1993).

[10] A. Fainstein *et al.*, Phys. Rev. Lett. **75**, 3764 (1995).

[11] A. Fainstein, B. Jusserand, and V. Thierry-Mieg, Phys. Rev. Lett. **78**, 1576 (1997).

[12] W. R. Tribe *et al.*, Phys. Rev. B **56**, 12 429 (1997).

[13] A. Fainstein, B. Jusserand, and R. André, Phys. Rev. B **75**, R9439 (1998).

[14] The conditions for polariton mediated doubly resonant Raman scattering can be realized also in II-VI structures. However, to the best of our knowledge this has not been reported experimentally.

[15] For more details on the samples see Refs. 3 and 4.

[16] A. I. Tartakovskii *et al.*, Phys. Rev. B **62**, R2283 (2000).

[17] The data presented in the paper are obtained from several samples with slightly differing values of negative detuning and Rabi splitting.

[18] The polariton energies show negligible temperature dependence (less than 1 meV) over the range 120–300 K.

[19] Daniel L. Akins, in *J Aggregates*, edited by T. Kobayashi (World Scientific, Singapore, 1996), pp. 67–93, and references therein.

[20] C. Weisbuch and R. G. Ulbrich, in *Light Scattering in Solids*, edited by M. Cardona and G. Güntherodt (Springer, Berlin, 1982), Vol. 3.

[21] The small asymmetry in the calculated cross section for the case of angle tuning arises from variation of the final state exciton fraction with ΔE_{DR}.

[22] A. Fainstein and B. Jusserand, Phys. Rev. B **57**, 2402 (1997).

[23] M. N. Shkunov *et al.*, Appl. Phys. Lett. **73**, 2878 (1998).

[24] H. Fider *et al.*, Chem. Phys. Lett. **171**, 529 (1990); Serdar Özçelik *et al.*, Appl. Phys. Lett. **73**, 1949 (1998).